

CHARACTERISATION OF WELD HETEROGENEITY THROUGH HARDNESS MAPPING AND MINIATURE TENSILE TESTING

J. Bally¹, W. De Waele¹, P. Verleysen², N. Gubeljak³ and S. Hertelé¹

¹ Ghent University, Laboratory Soete, Belgium

² Ghent University, Department of Materials Science and Engineering, Belgium

³ University of Maribor, Laboratory for Machine Parts and Structures, Slovenia

Abstract: Welding is a widely adopted industrial process used for joining components. A fusion weld has a highly heterogeneous microstructure and characterisation of strength heterogeneity is difficult because of the potentially large variations over a limited distance. Hardness mapping and miniature tensile tests are two distinct approaches to this problem. This paper reports on the possibilities and limitations of both techniques. Hardness mapping is a well-documented procedure as opposed to miniature tensile testing, where the dimensions of the dogbone shaped specimens are smaller than what standards prescribe. A particular challenge is the measurement of strains in such small specimens. The authors have achieved this measurement by means of Digital Image Correlation (DIC). To that end, a sufficiently fine speckling method has been developed.

Keywords: heterogeneity; hardness mapping; miniature tensile testing; DIC

1 INTRODUCTION

Welding is one of the most common joining methods due to its generally high production speed and low associated costs. It is often associated with flexibility, integrity and reliability [1]. An example application showing the economic importance of welding is pipeline installation. Costs associated to fusion welding are estimated to make up 20% of the total cost of pipe laying. These include aligning the pipe sections, cleaning and grinding, welding, checking the weld for flaws and coating the weld [2].

Notwithstanding the economical appeal of welding, the localized application of heat and melting results in a high susceptibility to material discontinuities, flaws and residual stresses, whose presence may lead to structural failure and lifetime reduction. The prediction of weld flaw acceptability ('structural integrity') is hampered by the potential presence of strongly heterogeneous microstructures. Modern day weld flaw assessment ignores this heterogeneity by assuming a homogeneous weld. As such, a generally accepted method to characterise weld heterogeneity does not yet exist.

2 STATE OF THE ART

Heterogeneity is inherent to fusion welds, because in order to melt the weld metal and fuse it with the base metal, heat has to be locally applied. For thicker sections, weldments are created in several passes (deposition of multiple layers), resulting in a variety of zones undergoing a succession of particular heat cycles. The heat cycle determines what the microstructure transforms into, each structure having a different stress-strain response. Not only the weld metal is heterogeneous due to this, but the heat affected zone (HAZ) of the base metal (heated but non-melted metal in close vicinity of the weld) also transforms.

Many conventional steel welds show a hardened HAZ due to the occurrence of stronger microstructures. In contrast, a broad range of high strength low alloy steels obtain their properties from a fine grain size, resulting from a specific heat treatment, often combined with mechanical deformation. These steels may show a softened HAZ due to grain coarsening. To quantify variations within weld metal and HAZ metal, two methods are considered in this paper: hardness mapping and miniature tensile testing

2.1 Hardness mapping

Several conversions between hardness values and various tensile parameters of a metal have been proposed [3]. However, these relations are material dependent and scattered. Given the heterogeneity of weldments, the accuracy of the correlations (developed for homogeneous materials) can be expected to drop. Homogeneous materials can be quantified more accurately by calculating averaged values based on multiple hardness measurements in identical material. This, however, is impossible for strongly heterogeneous materials. In addition, estimations of other constitutive parameters such as yield strength and strain hardening require material-specific assumptions (e.g. discussed in reference [4]). Nonetheless,

hardness maps provide an intuitive and qualitative view of weld strength heterogeneity in both dimensions of a weld cross section. Concretely, a grid of Vickers indents across the weld zone is made. According to ASTM E384-11, the minimum distance between the centers of adjacent indentations should be at least 2.5 times the diagonal of the expected minimum hardness (the lowest hardness indent will have the largest indent size) to avoid interactions between their regions of influence.

2.2 Miniature tensile testing

Local heterogeneity cannot be quantified with standard sized tensile specimens; the minimum width of the parallel length of a dogbone tensile test specimen in standard ASTM E8M-04 ('W' in Figure 1) is 6 mm. This is too large to determine local properties and the stress-strain curve obtained with such tensile tests will be an average of the collection of sampled zones.

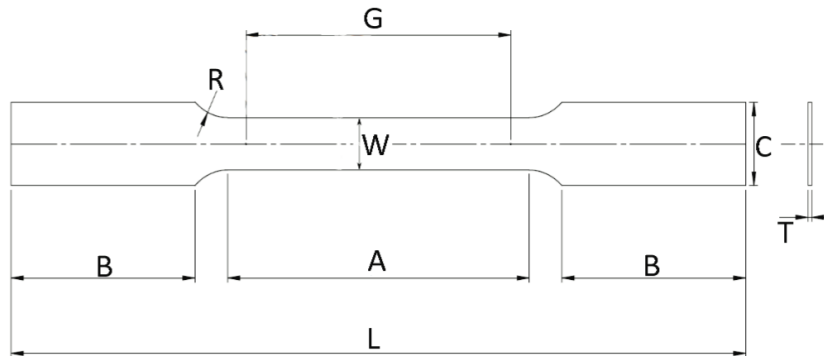


Figure 1. Schematic view of an ASTM E8M-04 tensile specimen: G-gauge length, W-width of parallel-zone, T-thickness, R- radius of fillet, L-overall length, A-length of reduced section, B-length of grip section, C- width of grip section [13].

A large number of research papers has been published, where these size limitations are discarded and so-called miniature tensile test specimens are used. This is typically associated with a width W of the reduced section of about 2 mm [1, 5-13]. As seen in Figure 2, which compares the result of such a miniature tensile test (cross section of the reduced section: 2 mm x 0.5 mm) of a homogeneous material to a standard sized tensile test of the same material, there are clear but reasonable deviations in the stress-strain curve. Properly characterizing the linear-elastic stage appears to be challenging. A major point of attention is the size effect with respect to defects. In smaller specimens, defects have more importance, as their size relative to the overall cross section dimensions is larger. These defects act as failure initiation sites and thereby tend to reduce the ultimate tensile strength. Even so, the tensile test data such as yield strength, ultimate tensile strength have been observed to deviate less than ten percent from their values in standard sized tests [11], which is considered sufficiently accurate to investigate the usefulness of this type of test.

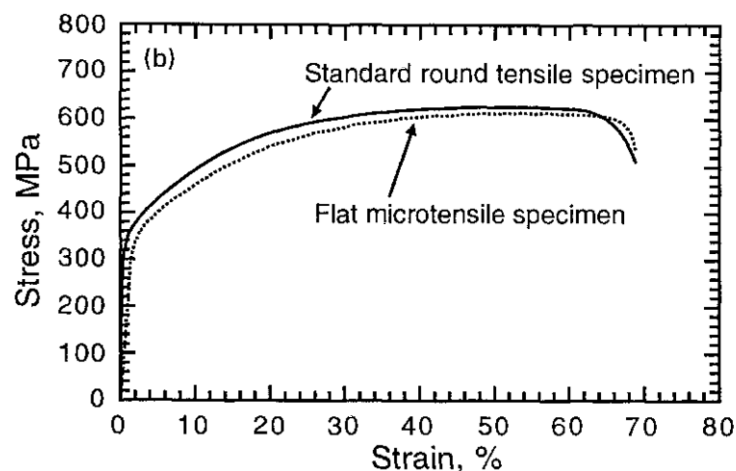


Figure 2. Comparison of stress-strain curves for base metals obtained by testing standard round and flat miniature tensile specimens of St 52 steel [11].

3 EXPERIMENTAL ACTIVITIES

3.1 Vickers hardness mapping

In order to characterise welds both hardness maps and miniature tensile tests are of interest. Two multi-pass shielded metal arc welds (SMAW) have been studied. They were extracted from an API 5L X60 pipeline, having operated in the field for 45 years. Figure 3 shows a grid of hardness indents (ca. 800 total) applied on a weld cross section of one of both welds on the left, and the corresponding hardness map on the right. An indentation mass of 5 kg was used ('HV5'). The spacing between indents was in agreement with ASTM E384-11. Clearly, the largest variation within the weld occurs in the through-thickness direction. Tensile properties will also show large variations in this direction, being slightly undermatched with respect to the base metal near the weld root, and strongly overmatched near the weld cap (in terms of ultimate tensile strength).

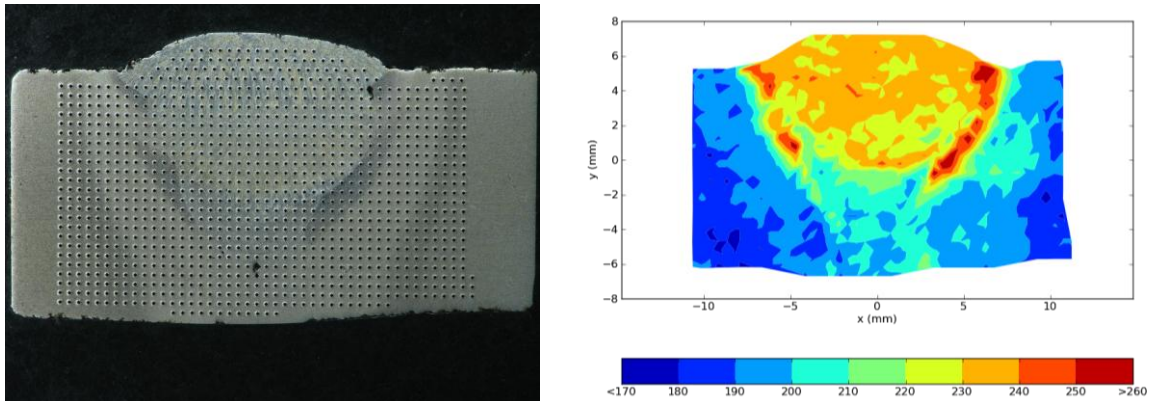


Figure 3. Left: Vickers hardness map of one of the welds. Right: weld sample after making the hardness map.

3.2 Tensile testing of miniature specimens

The most common method used to produce miniature tensile specimens is wire electro discharge machining ('wire EDM') [1, 7, 8, 10, 11, 13-17] (note that one study used water jet cutting [18]). The advantage of EDM over traditional machining processes is that it can produce the small work piece accurately and to close tolerances with very little wasted material. In the EDM process there is no physical contact between the tool and the work piece, which implies that the small work piece cannot break due to the force that would be applied by other methods. Finally, note that EDM requires an electrically conductive work piece, which clearly is not a concern in this case.

Concerning the geometry of a macro tensile test specimen, the standard ASTM E8M-04 prescribes certain ratios between the parameters in Figure 1. In an attempt to avoid that the boundary effects of the end shoulders influence the response of the test section, these ratios can be adopted for miniature tensile test specimens. In studies [17, 19] the importance of some of these ratios in miniature tensile test specimens is investigated. The consensus is that an important ratio is G/W and the best results are obtained when adhering to a ratio of 4, just as the standard prescribes for traditional specimens. This at least requires that $A/W \geq 4$ because the gauge length G is the distance between attaching points of a clip gauge, which has to be attached between the end points of the reduced section with length A . The dimensions used to obtain the dotted curve in Figure 2 are shown in the lower half of Figure 4. These are also the dimensions selected for this paper. Aside from study [11], several other independent studies, published by mostly different authors and including a study partially made at Soete Laboratory, use very similar dimensions [1, 5-10, 12, 13, 20]. A comparison of the exact dimensions used can be found in Table 1. Notably, B and A from reference [20] were not explicitly mentioned, but obtained from communication with the principal investigator of the test program. Studies [7, 10, 11, 13] show good agreement between the tensile test data acquired with these dimensions and tensile test data of full size specimens, both machined out of the same homogeneous material.

In this work, miniature tensile test specimens have been produced as follows. In the first production step a prism is extracted by EDM, using a 0.25 mm diameter wire, as shown in the top right of Figure 4. Its length is larger than that of the final specimens to allow for clamping during the next process step: 0.7 mm thick slices are machined, by letting the EDM wire follow an 'L' shaped path as indicated on the top right of Figure 4. The slices are further ground down to the final thickness of 0.5 mm to ensure adequate accuracy on the final thickness. Smaller dimensions increase the difficulty in manufacturing and handling of the specimens. The top left illustration in Figure 4 indicates the orientation of the specimens in the weld: they

are oriented in the direction of welding to confirm the variation in tensile properties suggested in Figure 3. EDM removes very little material between the slices, which means the ‘spatial resolution’ on the variation of the tensile properties throughout the weld thickness is high. The specimens have one rounded corner in one of the clamped sections of the dogbone, thus providing a ‘fool-proof’ reference to their orientation with respect to the weld.

	L (mm)	B (mm)	A (mm)	W (mm)	C (mm)	R (mm)	T (mm)	A/W (-)
[1, 5, 6, 8-11, 13]	21	4.5	9	2	5	1.5	0.5	4.5
[7]	25.6	6	8.6	2.4	8.9	3	1.3	3.6
[12]	10.65	2	5.65	2	3	0.5	0.5	2.8
[15]	10	2.5	3	1	4	1	1	3
[20]	25	5	8	2	5	3	0.5	4.0

Table 1. Comparison of miniature tensile test specimen dimensions, see Figure 1 for dimension labels. All dimensions in mm.

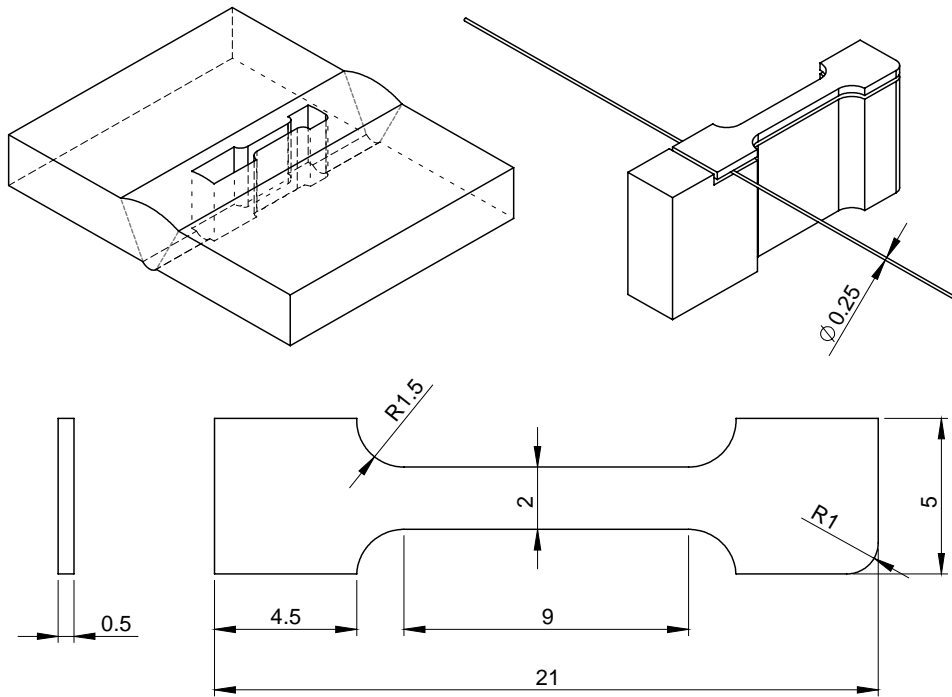


Figure 4. Extraction process of the specimens on top and their dimensions below. The arrow indicates the direction of the welding process. Dimensions are taken from [6] and differ only in the rounded corner.

The surface of the dog bones produced by EDM is expected to be fairly rough and to contain faults, notably a thin, brittle, hard layer (called the white layer) and a heat affected zone of up to 250 μm as observed in [21-23]. To minimise the influence of the surface defects and the altered grain structure after the wire EDM process, the flat surfaces of the dog bones have been polished using sand paper with very fine particles. Zhao et al. used 4000 grit SiC sandpaper in [16] and [17]. This polishing step reduced the surface roughness (and thus stress concentrations at the surface) from about 20 μm R_a to a value better than 0.045 μm R_a (as estimated from the R_q value) [24]. In the current study, 2000 grit sandpaper was used.

Figure 5 shows a miniature tensile specimen obtained in the framework of this research, after polishing with 2000 grit sandpaper. The measured roughness after polishing was around 0.03 μm R_a .

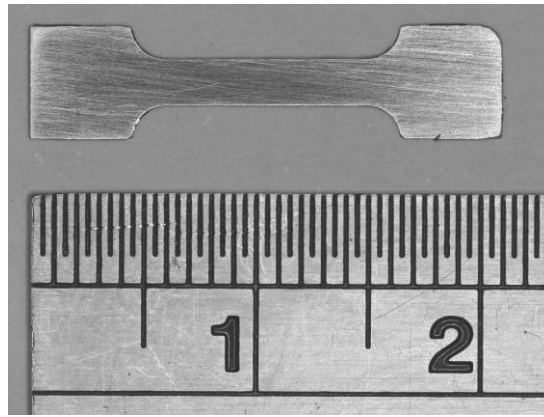


Figure 5. Miniature tensile specimen after polishing with 2000 grit sandpaper.

4 DIGITAL IMAGE CORRELATION

Measuring strain in a miniature tensile test specimen is difficult; attaching traditional strain gauges or extensometers is practically impossible. A method to estimate strain from the crosshead displacement has been investigated by Akbary et al. [25] using mathematical models to correct for the (elastic) deformations of the shoulder areas and of the machine itself. In parallel, strain was optically measured. Digital image correlation (DIC) was used and proved more accurate when compared to a full sized tensile test. Therefore, Soete Laboratory's three-dimensional DIC setup has been used to optically measure strains during miniature tensile testing. 3D DIC relies on pattern recognition: two monochromatic 5 MPx cameras simultaneously capture a random speckle pattern on the surface, having an optimal average speckle size of 3 by 3 camera pixels [26]. Devoted commercial software (VIC3D, Correlated Solutions Inc.) compares consecutive images taken during the loading process. Using correlation algorithms the deformation of the pattern from one image to the next is calculated. When the setup is properly calibrated three-dimensional deformations and, more importantly, surface strains can be calculated. Coupling back longitudinal strain to the applied force, a stress-strain-curve can be obtained.

The area of interest is about 15 mm long (taking into account that the gauge length of interest needs to be able to elongate from its original 9 mm length) and 2 mm wide. Considering that the camera resolution is 2500 by 2000 pixels, this implies a scale of 170 pixels per mm. The optimal speckle size then becomes 18 by 18 μm . In literature two methods are found to create speckle patterns of this size. One involves toner powder deposition and the other contact lithography; both are described in [26-28].

For this work, it was attempted to create a pattern with speckles of the desired small size with ordinary liquid paint. Paint droplets were sprayed on the surface through an airbrush nozzle. The general method involves using a small diameter airbrush nozzle, aiming the spray towards a piece of paper that's held at an angle to the surface that requires the speckle pattern. Very small paint droplets bounce off this paper, which has a thin layer of paint built up on it. After experimenting with the specifics of this method, speckle sizes were verified on a microscope. An example micrograph is shown in Figure 6.

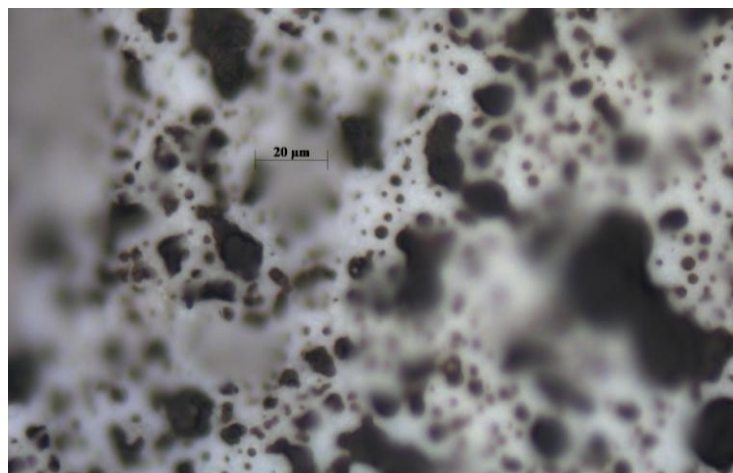


Figure 6. Example of a micrograph used to determine speckle sizes.

Based on the microscope study, some of the generated patterns with sufficiently different speckle sizes were selected to be compared by the DIC setup. They were photographed, displaced slightly by hand and then photographed again. The VIC3D software was used to correlate the subsequent photographs. The pattern with the lowest maximal σ value (a measure of the standard deviation of the image correlation) was selected as the optimal speckle generating method. Values below 0.03 are considered to be excellent [26]. Figure 7 shows a close-up of the chosen speckle pattern, which had the lowest maximal value: $\sigma = 0.034$. The pattern shows appropriate speckle size, clear contrast, sufficient speckle density, and is acceptably random. In Figure 8 the map of the σ values of the optimal pattern can be seen. It shows clear peaks on the right, corresponding with a decrease in speckle density of the pattern. With some additional practice, the density can be made more uniform, thereby slightly decreasing the maximal σ value.

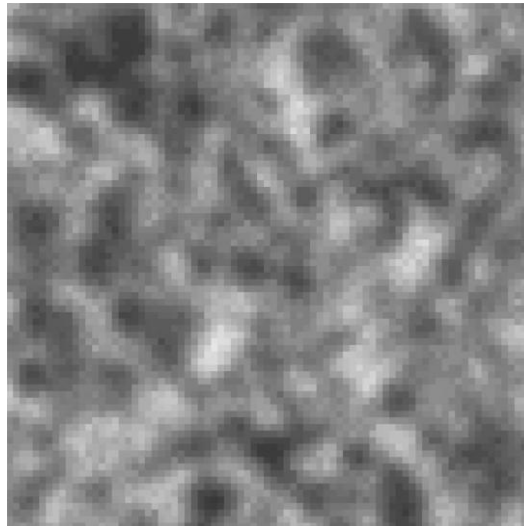


Figure 7. Close-up (80x80 pixels) of the speckle pattern, as seen by the DIC setup. 1 pixel is 6.8 μm by 6.8 μm .

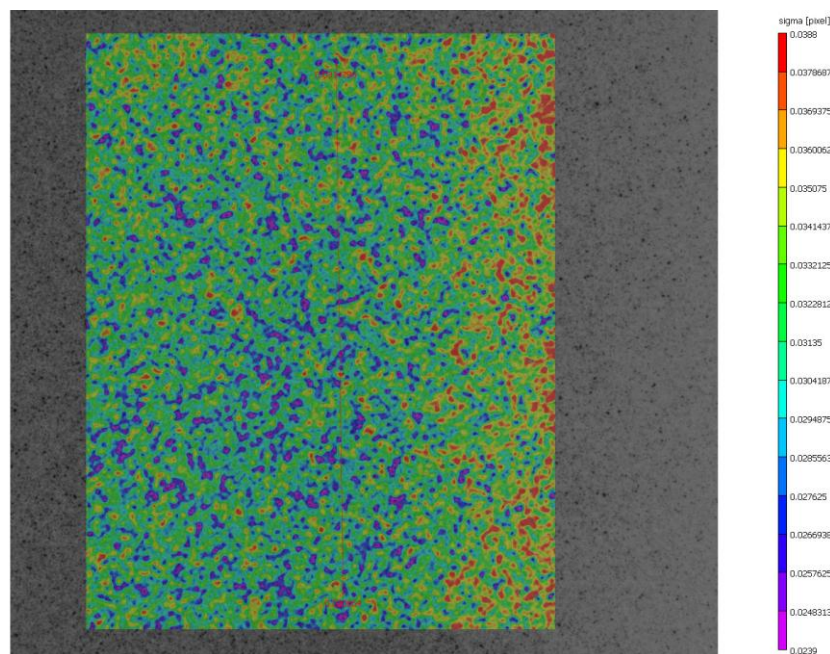


Figure 8. Map of standard deviation (" σ ") values of the correlated patterns.

Figure 9 shows an example strain distribution measurement during a miniature tensile test. The development of Lüders bands in the prismatic section – remote from the shoulders – is clearly observed and, from further quantitative analysis, local strain measurement accuracy was confirmed to be within $\pm 0.02\%$ strain (or 200 microstrain). Strain output towards the stress-strain curve was generated by means of a 'virtual extensometer' having a gauge length 8 mm (corresponding with $G/W = 4$ in Figure 1). Local strain measurement errors are averaged over this gauge length, resulting in a significantly lower extensometer

strain error. The in-depth discussion hereof is outside the scope of this paper. Overall, DIC proved to be more than sufficiently accurate from the viewpoint of obtaining reliable stress-strain curves, including the linear-elastic, plastic and post-necking stage.

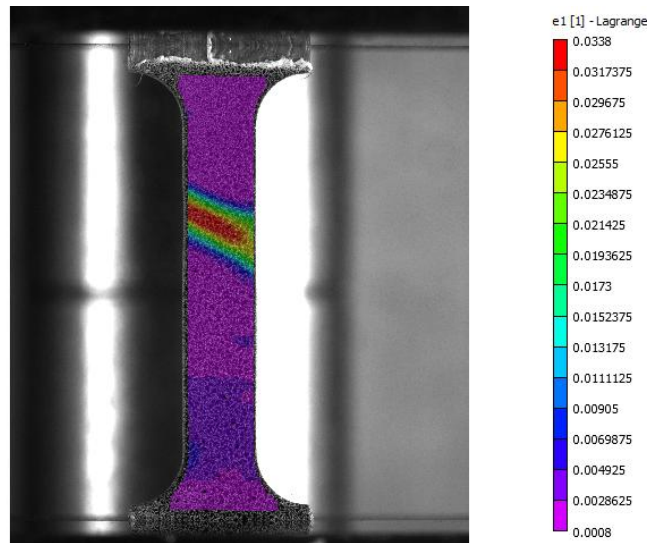


Figure 9. Example strain distribution measurement during a miniature tensile test, indicating the development of Lüders bands in the prismatic section.

5 CONCLUSIONS

In order to characterise weld heterogeneity and lay a foundation for more extensive consideration of the effects of this heterogeneity on overall weld performance, two characterisation methods were explored in this paper. The first, hardness mapping, is a well-established method, but is hampered by material specific conversion to tensile data. It does indicate general trends in strength variation. The second, miniature tensile testing, provides more specific and complete data. However, this method is not standardized, requiring experimentation with and verification of the method itself. This paper described how, at Soete Laboratory, both aspects have been investigated in detail and optimized where possible.

6 ACKNOWLEDGEMENTS

The authors would like to acknowledge the support of the Belgian Welding Institute (BIL-IBS) for creating the weld macrograph shown in Figure 3.

7 REFERENCES

- [1] Zerbst, U., et al., *Review on fracture and crack propagation in weldments – A fracture mechanics perspective*. Engineering Fracture Mechanics, 2014. **132**: p. 200-276.
- [2] Yapp, D. and S.A. Blackman, *Recent developments in high productivity pipeline welding*. Journal of the Brazilian Society of Mechanical Sciences and Engineering, 2004. **26**: p. 89-97.
- [3] ISO, *Metallic materials - conversion of hardness values (ISO 18265:2003)*. 2003.
- [4] Hertelé, S., et al., *Fracture Mechanics Analysis of Heterogeneous Welds: Validation of a Weld Homogenisation Approach*. Procedia Materials Science, 2014. **3**: p. 1322-1329.
- [5] Koçak, M. *Structural Integrity of Welded Structures: Process-Property-Performance (3P) Relationship*. in *63rd Annual Assembly & International Conference of the International Institute of Welding*. 2010.
- [6] Pakdil, M., et al., *Microstructural and mechanical characterization of laser beam welded AA6056 Al-alloy*. Materials Science and Engineering: A, 2011. **528**(24): p. 7350-7356.
- [7] Balakrishnan, K.S., et al., *Suitability of Miniature Tensile Specimens for Estimating the Mechanical Property Data of Pressure Tubes: An Assessment*. Transactions of the Indian Institute of Metals, 2014. **67**(1): p. 47-55.
- [8] Cam, G., et al., *Determination of mechanical and fracture properties of laser beam welded steel joints*. Welding Journal, 1999. **78**: p. 193-s.

- [9] Ceyhan, U., M. Horstmann, and B. Dogan, *High temperature cross-weld characterisation of steel weldments by microtensile testing*. *Materials at High Temperatures*, 2006. **23**(3-4): p. 233-243.
- [10] Dobi, D. and E. Junghans, *Determination of the tensile properties of specimens with small dimensions*. *Kovine Zlitine Tehnologije*(Slovenia), 1999. **33**(6): p. 451-457.
- [11] Çam, G., et al., *Investigation into properties of laser welded similar and dissimilar steel joints*. *Science and Technology of Welding and Joining*, 1998. **3**(4): p. 177-189.
- [12] Dedov, A. and I. Klevtsov, *Comparison of direct and indirect methods of tensile properties determination for post-exposed power plant steels*. *Annals of Danube Adria Association for Automation & Manufacturing for 2012 & Proceedings of the 23rd Internationaal DAAAM Symposium*, 2012. **23**(1): p. 95-98.
- [13] Wang, H.T., et al., *Local mechanical properties of a dissimilar metal welded joint in nuclear powersystems*. *Materials Science and Engineering: A*, 2013. **568**(0): p. 108-117.
- [14] LaVan, D.A. and W.N. Sharpe, Jr., *Tensile testing of microsamples*. *Experimental Mechanics*, 1999. **39**(3): p. 210-216.
- [15] Oelbrandt, W., *Microtests on nanomaterials, MSc thesis dissertation*. 2013: Ghent University.
- [16] Zhao, Y.H., et al., *Influence of specimen dimensions on the tensile behavior of ultrafine-grained Cu*. *Scripta Materialia*, 2008. **59**(6): p. 627-630.
- [17] Zhao, Y.H., et al., *Influence of specimen dimensions and strain measurement methods on tensile stress-strain curves*. *Materials Science and Engineering: A*, 2009. **525**(1-2): p. 68-77.
- [18] Wudtke, I., et al., *A hierarchical multi-scale approach to mechanical characterization of heat affected zone in welded connections*. *Computational Materials Science*, 2015. **96, Part B**: p. 396-402.
- [19] Pierron, O.N., D.A. Koss, and A.T. Motta, *Tensile specimen geometry and the constitutive behavior of Zircaloy-4*. *Journal of Nuclear Materials*, 2003. **312**(2-3): p. 257-261.
- [20] Hertelé, S., N. Gubeljak, and W. De Waele, *Advanced characterization of heterogeneous arc welds using micro tensile tests and a two-stage strain hardening ('UGent') model*. *International Journal of Pressure Vessels and Piping*, 2014. **119**: p. 87-94.
- [21] Ekmekci, B., *Residual stresses and white layer in electric discharge machining (EDM)*. *Applied Surface Science*, 2007. **253**(23): p. 9234-9240.
- [22] Kruth, J.P., et al., *Study of the White Layer of a Surface Machined by Die-Sinking Electro-Discharge Machining*. *CIRP Annals - Manufacturing Technology*, 1995. **44**(1): p. 169-172.
- [23] Rebelo, J.C., et al., *Influence of EDM pulse energy on the surface integrity of martensitic steels*. *Journal of Materials Processing Technology*, 1998. **84**(1-3): p. 90-96.
- [24] Tabenkin, A. *To each his own parameter*. 2000 [visited 22/01/2015]; Available from: <http://www.qualitydigest.com/june01/html/surface.html>.
- [25] Hajy Akbary, F., M.J. Santofimia, and J. Sietsma, *Elastic Strain Measurement of Miniature Tensile Specimens*. *Experimental Mechanics*, 2014. **54**(2): p. 165-173.
- [26] Sutton, M.A., J. Orteu, and H.W. Schreier, *Image correlation for shape, motion and deformation measurements*. p. 233-236, 240-242. 2009: Springer Science and Business Media.
- [27] Scrivens, W.A., et al., *Development of Patterns for Digital Image Correlation Measurements at Reduced Length Scales*. *Experimental Mechanics*, 2007. **47**(1): p. 63-77.
- [28] Sutton, M.A., et al., *Local crack closure measurements: Development of a measurement system using computer vision and a far-field microscope*. *ASTM Special Technical Publication*, 1999. **1343**: p. 145-156.